IEEE Photonics Journal
An IEEE Photonics Society Publication

Open Access

Dissipative Soliton Resonance in an All-Polarization Maintaining Fiber Laser With a Nonlinear Amplifying Loop Mirror

Volume 12, Number 3, June 2020

Qihang Gong
Haitao Zhang
Decai Deng
Jiaqi Zu

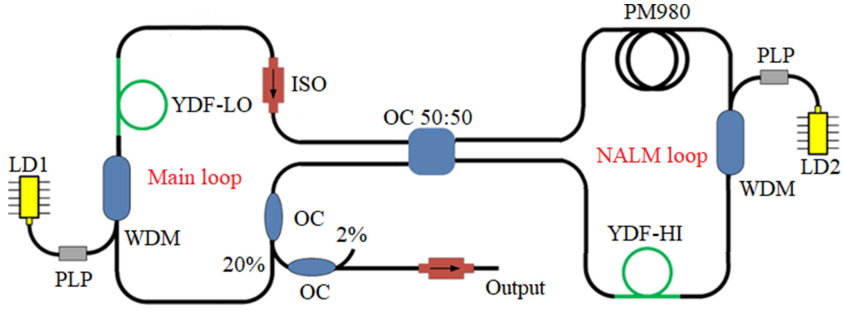

DOI: 10.1109/JPHOT.2020.2993695

Dissipative Soliton Resonance in an All-Polarization Maintaining Fiber Laser With a Nonlinear Amplifying Loop Mirror

Qihang Gong, Haitao Zhang, Decai Deng, and Jiaqi Zu

Key Laboratory of Photonic Control Technology, Tsinghua University, Ministry of Education, Beijing 100084, China

DOI:10.1109/JPHOT.2020.2993695

Manuscript received January 13, 2020; revised May 1, 2020; accepted May 6, 2020. Date of publication May 11, 2020; date of current version May 26, 2020. This work was supported in part by Key Basic Research Program for Basic Enhancement of Scientific and Technological Commission and in part by the National Natural Science Foundation of China under Grant 61475081. Corresponding author: Haitao Zhang (e-mail: zhanghaitao@mail.tsinghua.edu.cn).

Abstract: An all-polarization maintaining mode-locked Yb-doped fiber integrated laser with a nonlinear amplifying loop Mirror (NALM) under the operation regime of dissipative soliton resonance (DSR) has been demonstrated. The mode-locked laser can generate DSR pulses at 1.04 μm at the repetition rate of 2.59 MHz. The output DSR pulses can be tuned in pulse width from hundreds of picoseconds to a few nanoseconds by adjusting the pump power. By changing the pump power of the main loop and the NALM, the maximum output average power of 51.4 mW and the corresponding pulse energy about 20 nJ are achieved, respectively. Pulse breaking of the DSR pulses was observed apart from the typical pulse broadening at a fixed pulse peak power due to the peak power clamping effect, while solely increasing the main loop pump power. In addition, the characteristics of the DSR pulses such as pulse width, pulse energy, output power and optical spectrum with the changing of main loop pump power and NALM pump power are also discussed respectively.

Index Terms: Dissipative soliton resonance, nonlinear amplifying loop mirror, fiber laser.

1. Introduction

Generating high energy laser pulses from a passive mode-locked fiber laser is a challenging task since it is limited by soliton area theorems and spectral sideband which lead to pulse breaking with high pump power [1], [2]. In order to refrain pulse breaking, a new dissipative soliton mechanism, dissipative soliton resonance (DSR), is proposed to achieve a higher energy output [3]–[8]. The DSR pulse can achieve tens of nanojoules energy which is much higher than conventional solitons [9]–[11]. Akhmediev *et al.* firstly predicted the generation of ultra-high energy in theory as a certain solution of the complex cubic-quintic Ginzburg–Landau equation [12]. Soon afterwards, Chang *et al.* proposed the concept of dissipative soliton resonance (DSR) [13]. Due to the peak power clamping effect, the DSR output pulse width broadens linearly with pulse energy without any pulse breaking, keeping the peak power to remain constant. This means the output energy can be infinitely high with an ultra-wide pulse [13]. Later, other experiments also demonstrated that the generation of DSR is independent of normal or anomalous dispersion region and mode-locked

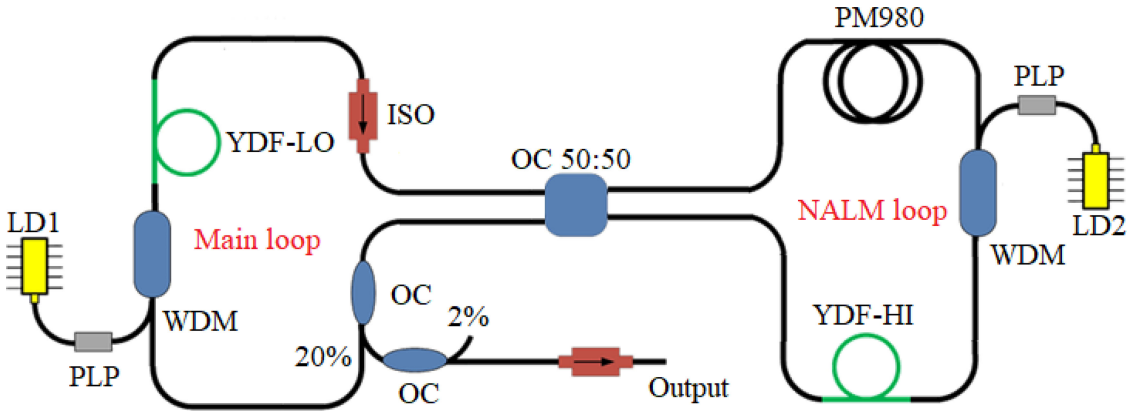

Fig. 1. Schematic of the DSR laser system. LD: laser diode; WDM: wavelength division multiplexers; OC: output coupler; and PLP: pump laser protector.

technique [14]–[17]. And the DSR is easy to self-start and all-fiber structure provides high reliability and small size and low weight.

As a reliable, self-start mode-locked technique, nonlinear amplifying loop mirror (NALM) under the operation regime of DSR get more and more attention. Wang *et al.* demonstrated a 1.55 μm, 3.25 nJ DSR output by using NALM technique for the first time [16]. And then Lin *et al.* reported a 1038 nm 4.8 nJ DSR output in a Yb-doped fiber NALM laser. In particular, through adjusting the polarization controllers, the DSR can be wavelength-tuned in a wide range. However the configuration is not all-polarization maintaining. [18]. Recently, Xu *et al.* demonstrated numerical simulation about the DSR in an all-normal-dispersion dual-pump mode-locked fiber laser based on a NALM [19]. Their works reveal that the utilization of NALM could effectively enlarge the saturable power as well as the transmittivity, which provide a road to increase the DSR peak power [19]. However, most of current works are concerned about Er-doped fiber laser in 1.5 μm wavelength, and there are few reports about DSR in an all-polarization maintaining Yb-doped fiber laser with a NALM operating at 1 μm.

In this letter, we report an all-polarization maintaining mode-locked Yb-doped fiber integrated laser with a NALM under the operation regime of DSR. This is, to the best of our knowledge, the first time to achieve DSR pulses at 1.04 μm by an all-polarization maintaining fiber laser with nonlinear amplifying loop. The output DSR pulses can be tuned in pulse width from hundreds of picoseconds to a few nanoseconds by adjusting the pump power and the maximum output energy is up to 20 nJ. The use of this passive mode-locked fiber laser to generate rectangular pulses has significant advantages: (1) All-fiber structure with high reliability. (2) No modulator or complicated delay control device and easier to integrate. (3) The pulse width is continuously tunable. (4) The all PM fiber configuration provide an excellent stability and the polarized laser pulse usually has a high signal-to-noise ratio (SNR) in sensing field, leading to a relatively higher precision. And the configuration provides a novel method to obtain linearly-polarized ultrafast laser at flexible pulse width which could be widely used in optical communication [20], [21], material processing [22] and remote sensing [23], [24].

2. Experiment Setup

The all-PM fiber laser is schematically shown in Fig. 1 The laser cavity is built in a figure 8 configuration. A NALM loop, which acts as a saturable absorber (SA) to obtain mode-locking, is coupled into the main loop (a unidirectional ring) through a 50:50 fiber coupler (OC). The NALM loop include a 75 m long PM passive fiber (Nufern, PM-980-HP) and 0.5 m high-concentration Yb-doped PM fiber(Nufern, PM-YSF-HI-HP) pumped by a 976 nm laser diode (LD) using a 976/1030

nm wavelength-division-multiplexer (WDM). The main loop is composed of 1 m low-concentration Yb-doped PM fiber(Nufern, PM-YSF-LO-HP) acting as the gain medium which is also pumped by a 976 nm LD connected with a pump laser protector(PLP), a PM isolator to ensure the unidirectional operation and prevent backwards reflections and an 80% fiber output coupler (OC) to output laser. The output coupler is connected with another 2:98 OC, which the 2% output port is used to monitor the laser pulse in real time. The total length of laser cavity is estimated as 80 m corresponding to the repetition rate of 2.59 MHz. And the net cavity dispersion at 1030 nm is estimated to be 1.88 ps^2 in all-normal-dispersion region.

In this configuration, the phase shift φ between the clockwise and anticlockwise propagating pulses in NALM loop is adjusted by changing the pump power, relatively long PM-SMF fiber and high enough pump power LD are used. And the self-started mode-locking can operate in DSR regime by adjusting the main loop pump power and NALM pump power appropriately. The temporal characterization of the output was take using a photodetector (New Focus Model-1414, 25 GHz bandwidth) with an oscillator (Agilent 86100A-86106A, 40 GHz bandwidth). The optical spectral data was characterized using an optical spectral analyzer (Yokogawa AQ6370, 0.02 nm resolution). The RF spectrum was taken using a RF signal analyzer (Keysight N9040B, 1GHz bandwidth) incorporated with the above fast photodetector. And an autocorrelator (APE Pulse Checker, 30 ps span range) was used to analyze the autocorrelation trace.

3. Experiment Results and Discussion

In our experiment, by appropriately increasing the main loop pump power and the NALM loop pump power, self-started DSR mode-locking state can be easily obtained at the main loop pump power of 25 mW and NALM pump power of 72 mW. Fig. 2 shows the characteristics of the DSR pulse. As shown in Fig. 2a, the laser generates a stable train of pulses with an interval of ∼386 ns corresponding to the repetition rate of 2.59 MHz. The Fig. 2(b) shows the rectangular single pulse temporal profile with the pulse width of ∼288 ps. The inset in Fig. 2(b) shows the auto-correlation trace obtained with an autocorrelator (APE Pulse Checker) for a width scan range of 30 ps. As the scanning range of the autocorrelator is significantly narrower than the pulse duration, only a constant line can be observed in the autocorrelation trace. The auto-correlation trace does not show any pulse, spike or other fine structure over 30 ps window and there are not any unstable states observed. All of these confirm the laser operates in DSR regime instead of noise like pulse (NLP) state. And the signal-to-noise ratio (SNR) is about 75 dB, indicating very high temporal stability, as shown in Fig. 2(c). The inset also verifies the repetition rate is 2.59 MHz. Fig. 2(d) shows the measured optical spectrum. The central wavelength is 1039.48 nm with a 151 pm full width at half maxima (FWHM) spectral bandwidth. The simulation study of the DSR pulse in passively mode-locked all-normal-dispersion fiber lasers by Li et al [25] has shown the characteristics of optical spectrum. Due to the periodic change of the transmission, the optical spectrum of NALM is bell-shaped. And case for monotonic saturable absorber is flat in the center and has two high peaks in both sides. The experiment results tallies well with the simulation results. The optical spectrum shows the newly generated energy is accumulated more in central part of the optical spectrum than the edges, thus, the spectral filtering effect induced pulse breaking is circumvented [25]. Because the optical spectrum of the DSR pulse is very narrow, the corresponding pulse width of transform-limited pulse is very wide. And we can calculate the dispersion needed to de-chirp the pulse is 10^3 ps^2 order of magnitude. Conventional compression methods cannot provide such a large amount of dispersion. Furthermore, the chirp of the DSR pulse is highly nonlinear, which also increases the difficulty of compression. So the DSR pulse was not compressed in this letter.

Once single stable DSR pulse is achieved, increasing the NALM pump power will increase the pulse width with the constant peak power which is fully consistent with the DSR theory. As shown in Fig. 3(a), while keeping the main loop pump power 25 mW constantly, the pulse width and the output power increase linearly with the increasing of NALM pump power. As the pump power is increased from 72 mW to 284 mW, pulse duration is tuned from ∼288 ps to ∼1.38 ns corresponding

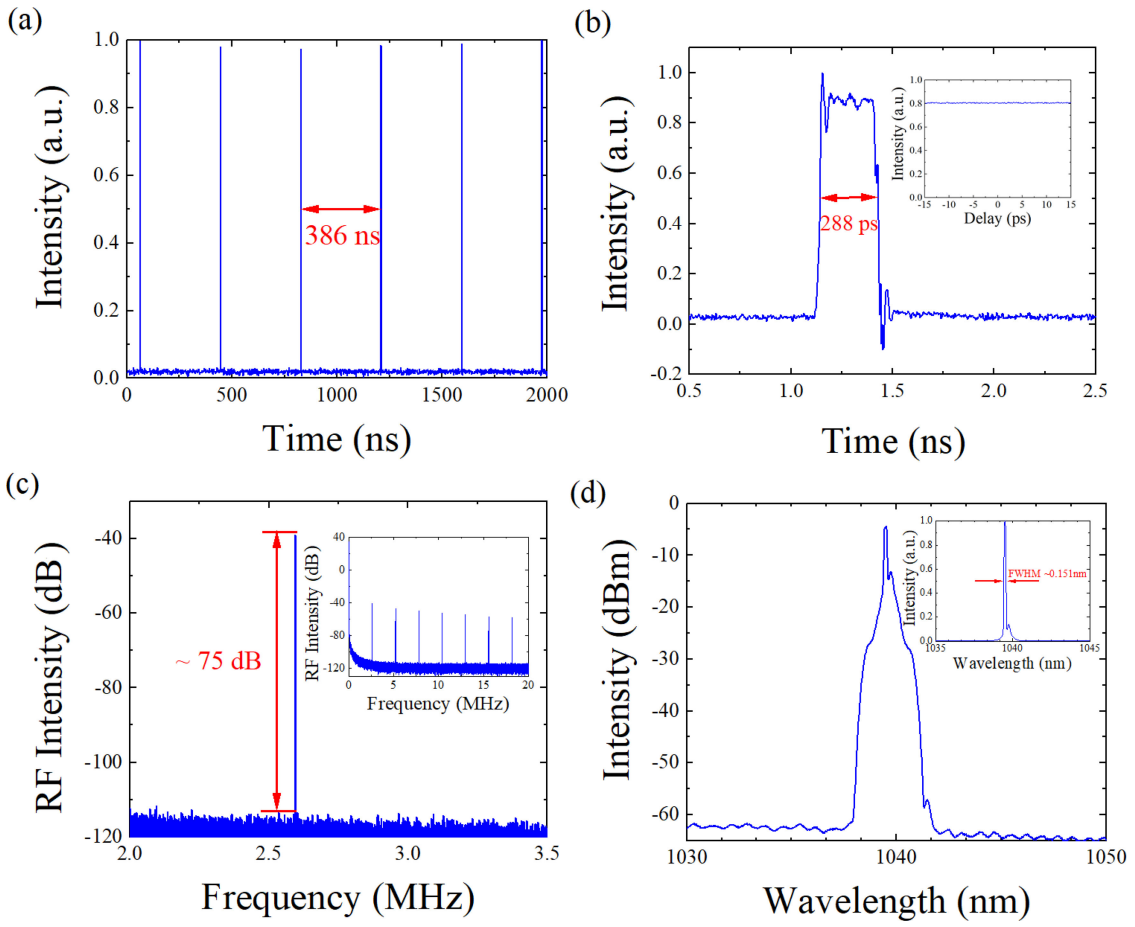

Fig. 2. Characteristics of the DSR pulse. (a) Pulse train. (b) Oscilloscope trace of a single pulse. Inset: Autocorrelation trace of the pulse. (c) RF spectra of the DSR output around the fundamental repetition rate. Inset: RF spectra of harmonic repetition rates. (d) Optical spectrum of the pulse with a log scale. Inset: Corresponding optical spectrum with a linear scale.

to the output power range from 6.1 mW to 51.4 mW. Considering pulse duration, repetition rate and the average power we can calculate the pulse energy and corresponding peak power. Fig. 3(b) presents the dependence of the pulse energy and corresponding peak power on the NALM pump power. The pulse energy is increased almost linearly from 2.4 nJ to 19.8 nJ. The peak power increased at first but then is clamped to ~14 W due to the peak power clamping effect induced by the periodic saturable absorption in NALM configuration. As shown in Fig. 3(c), while the DSR pulse became increasingly wider, the pulse profile remained rectangular and all of them have a higher front edge. Although the pulse width is broadened, there is not any pulse-breaking phenomena was observed. The inset shows the radio frequency (RF) spectrum of DSR pulse with 1.2 GHz span while pulse duration is 1.38 ns. The envelope of the RF spectrum is like a Sinc function, that is, the Fourier transform of a rectangular function. The figure exhibits a characteristic modulation with a period of 727 MHz corresponding to the duration of 1.38 ns. It also proved that the output DSR was indeed a rectangular pulse in the time domain. Fig. 3(d) shows the evolution of the optical spectrum. The spectral intensity is obviously increased, and the central wavelength is lightly blue shifted from 1039.48 nm to 1039.34 nm. The FWHM spectral bandwidth remained almost constant shifting from 151 pm to 145 pm, without any intra-cavity bandpass filters. It is worth noting that all above the results completely conform the DSR theory.

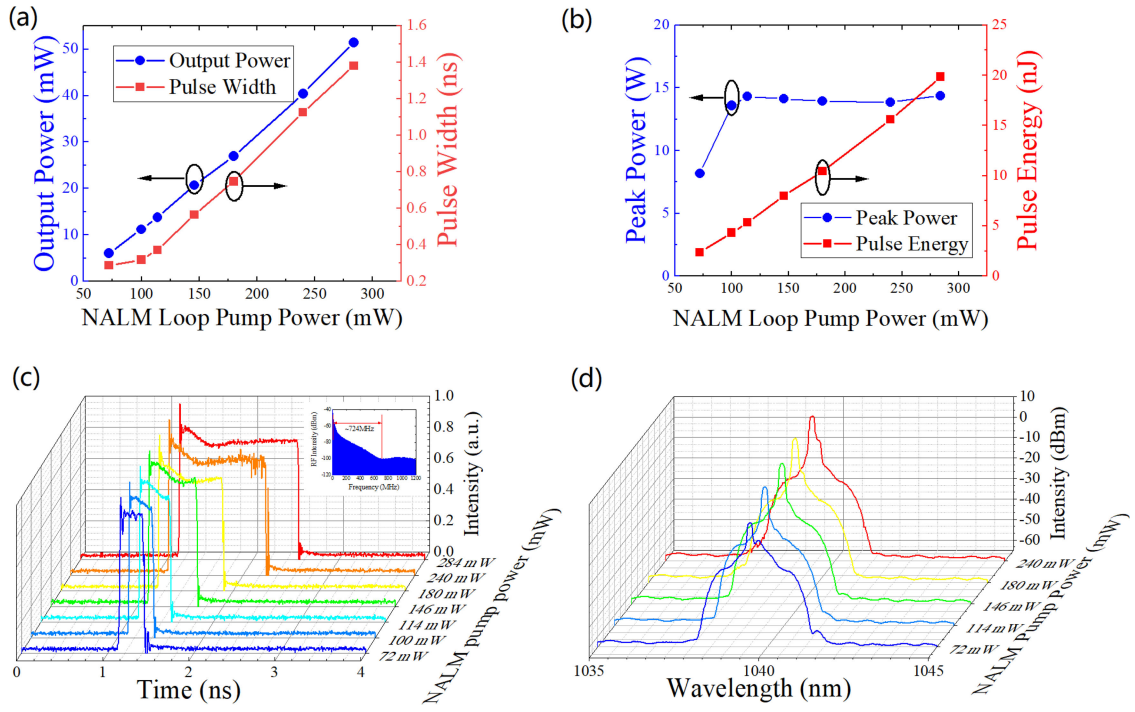

Fig. 3. Pulse broadening in the DSR regime (a) Pulse width and output power versus NALM loop pump power (red line for the pulse width, blue line for the output power). (b) Pulse energy and peak power versus the NALM loop pump power (red line for the pulse energy, blue line for the peak power). (c) Dynamics of pulse broadening in the time domain. Inset: RF spectra with1.2 GHz span. (d) Corresponding optical spectrum evolution.

The results have shown the configuration could generate stable DSR pulse and wave breaking is not observed while only increasing the NALM loop power. However, by only increasing the main loop power, the single-pulse DSR will transform into a dual-pulse and even tri-pulse state, as shown in Fig. 4. When the NALM loop power is fixed at 196 mW, increasing the main loop pump power to 123 mW, the single-pulse will evolve into a dual-pulse, as shown in Fig. 4(a), (b). The two sub-pulses have the almost same characteristics with similar pulse duration and amplitude. The sub-pulse interval is approximately 9.69 ns as shown in Fig. 4(a). Fig. 4(b) shows the first pulse profile and the pulse train of the dual-pulse. The rectangular sub-pulse with ~479 ps duration indicates the laser still operates in DSR regime and the interval of each dual-pulse is also ~386 ns corresponding to the same repetition rate of 2.59 MHz. When main loop pump power is further increased into 177 mW, the dual-pulse evolve into a tri-pulse state and the structure of the tri-pulse does not change significantly with the increase in the main loop pump power from 177 mW to 250 mW. Fig. 4(c) shows a typical tri-pulse profile with the main loop power of 224 mW. Three sub-pulses are also similar to each other. The interval between each sub-pulse is 9.69 ns and 10.15 ns. It is noticeable that the interval of the first and the second sub-pulse is same as the that of the dual-pulse, indicating that only the first two sub-pulse is evolved from dual-pulse. Fig. 4(d) shows the rectangular sub-pulse temporal profile with the pulse duration of ~788 ps and the pulse train with fundamental repetition rate. The tri-pulse is relatively stable in a large scale of pump power, but by increasing the main loop pump power up to 251 mW, the tri-pulse with small interval suddenly transformed into a tri-pulse with lager interval, as shown in Fig. 4(e). Although the sub-pulse still has the same profile, the interval of each other is increased largely to 19.32 ns and 42.78 ns. Fig. 4(f) shows sub-pulse is broadband to ~903ps. The three sub-pulses with different amplitude in the inset is due to the lack of sampling points and Fig. 4(e) proved three sub-pulses have the same amplitude. Fig. 4(g) shows the evolution of the above process. And the inset shows

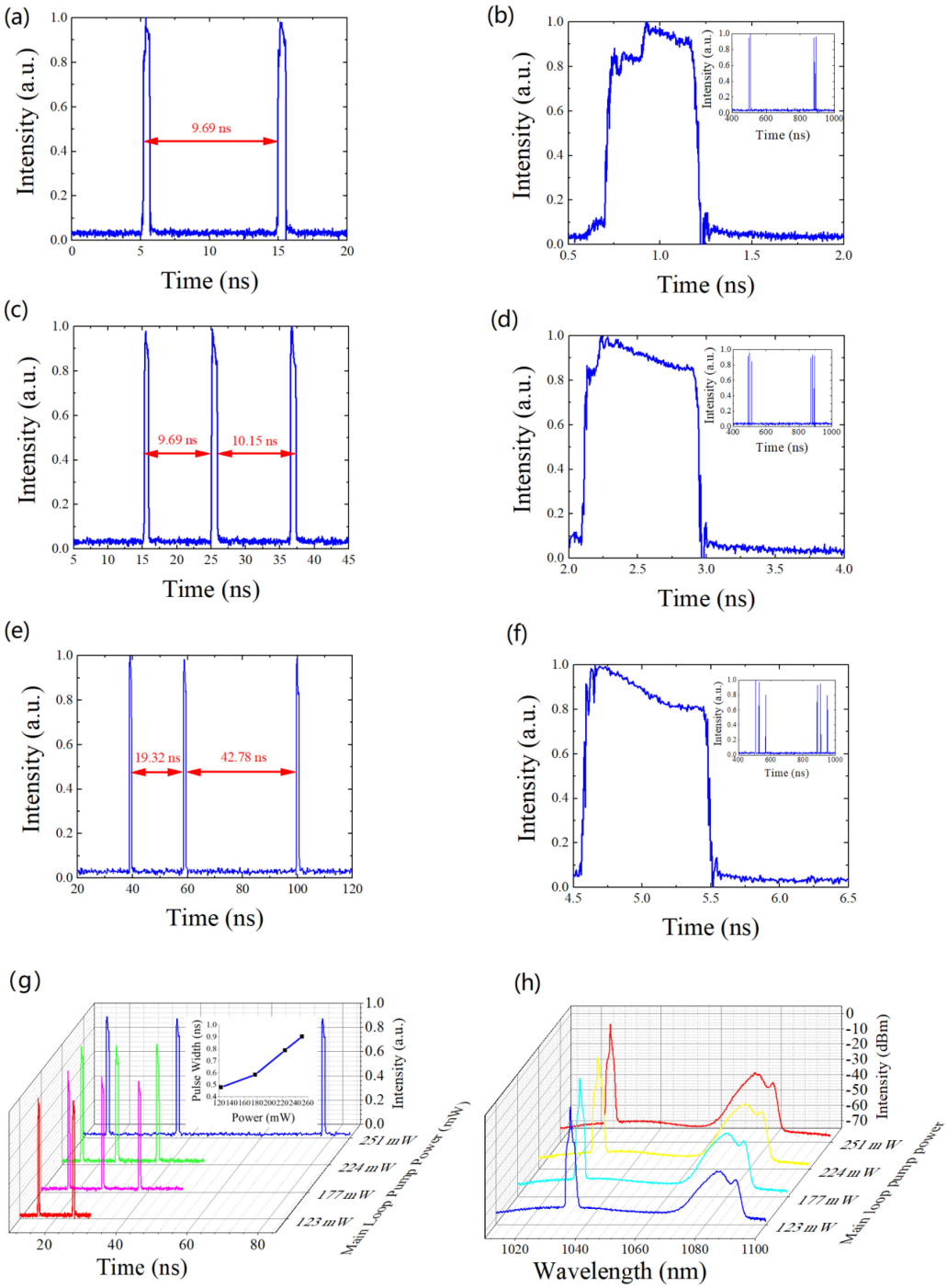

Fig. 4. Evolution of pulse broadening. (a) Oscilloscope trace of a dual-pulse. (b) Temporal profile of the sub-pulse in the dual-pulse. Inset: pulse train of the dual-pulse. (c) Oscilloscope trace of a tri-pulse with small interval. (d) Corresponding temporal profile of the sub-pulse in the tri-pulse. Inset: pulse train of the tri-pulse with small interval. (e) Oscilloscope trace of a tri-pulse with large interval. (f) Corresponding temporal profile of the sub-pulse in the tri-pulse. Inset: pulse train of the tri-pulse with large interval. (g) Dynamics of pulse breaking with increasing main loop pump power in the time domain. Inset: sub-pulse width versus main loop pump power. (h) Corresponding optical spectrum evolution.

relationship between the sub-pulse width and the increasing of main loop pump power. The less increase of pulse width between the dual-pulse and the first tri-pulse is due to the new generated third sub-pulse extract part of energy. And it is obviously that the pulse width is also increased linearly with the increasing of the pump power, which agrees well with the DSR theory. Fig. 4(h) shows the evolution of the optical spectrum. The signal near 1080 nm is due to the stimulated Raman scattering (SRS) effect. In order to obtain high nonlinear gain, a long SMF was used in the configuration, leading to the low threshold for the SRS. The spectral intensity is significantly increased, and the central wavelength is also blue shifted from 1034.96 nm to 1026.72 nm. The FWHM spectral bandwidth is almost fixed at 300 pm in the process.

The configuration of the laser is all-polarization maintained which means the polarization is almost fixed in the fiber. In some of other configurations, the polarization was adjusted which could suppress the pulse breaking. Furthermore, due to the relatively low repetition rate and high main loop pump power, the energy of soliton is high, which means it is easy to split before it is transformed to DSR in the NALM loop. It is remarkable that the intervals of the sub-pulse: 9.69 ns, 10.15 ns,19.32 ns, 42.78 ns corresponding to repetition rates 103.17 MHz, 98.50 MHz, 51.75 MHz, 23.37 MHz are integer multiple of fundamental repetition rate (40 times, 35 times, 20 times, 9 times). This suggests that the laser has possibility to operate in harmonic mode-locking (HML) in a dissipative soliton resonance (DSR) region [26], [27]. But the fiber in configuration is all-PM without any polarization controllers, thus, the polarization could not be tuned and the HML is not observed. In this configuration, the NALM loop played a role of saturable absorber and transformed the DS into the DSR region. So, increasing the NALM pump power will only increase the pump power of DSR pulse and in theory, the DSR pulse is pulse-breaking-free. In order to generate multi-pulse, the pulse should break before it is transformed into DSR pulse in the NALM loop. In other words, the only way is to increase the main loop pump power to make the soliton split. The generated dissipative soliton (DS) in the main loop firstly split into multiple DSs due to a relatively high pump power and are accumulated nonlinearity, and then these DSs are evolved into DSR pulses due to the appropriate cavity parameters. Increasing the pump power leads to the growth in number of solitons, this explain the how single-pulse DSR transform into dual-pulse or tri-pulse state. And generality, the multiple DSs are randomly spaced in the cavity, so the interval of each sub-pulses is not equal and even changes in different conditions.

4. Conclusion

In conclusion, we have experimentally demonstrated the 1040nm polarized DSR pulse in all-normal-dispersion fiber laser based on a NALM. A long SMF was inserted into the NALM loop to obtain high nonlinear gain. The appropriate parameters enable a high temporal stable DSR pulse with 2.59 MHz repetition rate. The pulse duration can be tuned from 288 ps to 1.38 ns with maximum 20 nJ pulse energy by increasing the NALM loop pump power. In addition, by only increasing the main loop pump power, pulse breaking is observed, which may be useful in sensing field. The results show that even the DS is split into multiple DSs, the sub-pulse will also transform into DSR pulse, which may be helpful to understand the DSR dynamics in the all-normal-dispersion PM fiber. The configuration could provide a promising way to generate polarized DSR pulse around 1 μm in a compact and low-cost fiber laser.

References

[1] L. E. Nelson, D. J. Jones, K. Tamura, H. A. Haus, and E. P. Ippen, "Ultrashort-pulse fiber ring lasers," *ApPhB*, vol. 65, no. 2, pp. 277–294, Aug. 1997, doi: 10.1007/s003400050273.

[2] X. Wu, D. Y. Tang, L. M. Zhao, and H. Zhang, "Effective cavity dispersion shift induced by nonlinearity in a fiber laser," *Phys. Rev. A*, vol. 80, no. 1, Jul. 2009, Art. no. 013804, doi: 10.1103/PhysRevA.80.013804.

[3] I. Armas-Rivera *et al.*, "Dissipative soliton resonance in a full polarization-maintaining fiber ring laser at different values of dispersion," *Opt. Express*, vol. 24, no. 9, pp. 9966–9974, May 2016, doi: 10.1364/OE.24.009966.

[4] S. Smirnov, S. Kobtsev, A. Ivanenko, A. Kokhanovskiy, A. Kemmer, and M. Gervaziev, "Layout of NALM fiber laser with adjustable peak power of generated pulses," *Opt. Lett.*, vol. 42, no. 9, pp. 1732–1735, May 2017, doi: 10.1364/OL.42.001732.
[5] W. Pan, J. Zhou, L. Zhang, and Y. Feng, "Rectangular pulse generation from a mode locked Raman fiber laser," *J. Light. Technol.*, vol. 37, no. 4, pp. 1333–1337, Feb. 2019.
[6] R. Becheker *et al.*, "Dissipative soliton resonance in a mode-locked Nd-fiber laser operating at 927nm," *Opt. Lett.*, vol. 44, no. 22, pp. 5497–5500, Nov. 2019, doi: 10.1364/OL.44.005497.
[7] Z. Zheng, D. Ouyang, X. Ren, J. Wang, J. Pei, and S. Ruan, "0.33mJ, 104.3W dissipative soliton resonance based on a figure-of-9 double-clad Tm-doped oscillator and an all-fiber MOPA system," *Photon. Res.*, vol. 7, no. 5, pp. 513–517, May 2019, doi: 10.1364/PRJ.7.000513.
[8] Y. Guo, Y. Xu, J. Zhang, and Z. Zhang, "High-power dissipative soliton resonance fiber laser with compact linear-cavity configuration," *Optik*, vol. 181, pp. 13–17, Mar. 2019, doi: 10.1016/j.ijleo.2018.10.127.
[9] D. A. Dvoretskiy *et al.*, "High-energy, sub-100 fs, all-fiber stretched-pulse mode-locked Er-doped ring laser with a highly-nonlinear resonator," *Opt. Express*, vol. 23, no. 26, pp. 33295–33300, Dec. 2015, doi: 10.1364/OE.23.033295.
[10] J. Wang *et al.*, "High energy soliton pulse generation by a magnetron-sputtering-deposition-grown MoTe2 saturable absorber," *Photon. Res.*, vol. 6, no. 6, pp. 535–541, Jun. 2018, doi: 10.1364/PRJ.6.000535.
[11] H. Yu, X. Wang, P. Zhou, X. Xu, and J. Chen, "High-energy square pulses in a mode-locked Yb-doped fiber laser operating in DSR Region," *IEEE Photon. Technol. Lett.*, vol. 27, no. 7, pp. 737–740, Apr. 2015, doi: 10.1109/LPT.2015.2390911.
[12] N. Akhmediev, J. M. Soto-Crespo, and Ph. Grelu, "Roadmap to ultra-short record high-energy pulses out of laser oscillators," *Phys. Lett. A*, vol. 372, no. 17, pp. 3124–3128, Apr. 2008, doi: 10.1016/j.physleta.2008.01.027.
[13] W. Chang, A. Ankiewicz, J. M. Soto-Crespo, and N. Akhmediev, "Dissipative soliton resonances," *Phys. Rev. A*, vol. 78, no. 2, Aug. 2008, Art. no. 023830, doi: 10.1103/PhysRevA.78.023830.
[14] W. Chang, J. M. Soto-Crespo, A. Ankiewicz, and N. Akhmediev, "Dissipative soliton resonances in the anomalous dispersion regime," *Phys. Rev. A*, vol. 79, no. 3, Mar. 2009, Art. no. 033840, doi: 10.1103/PhysRevA.79.033840.
[15] P. Grelu, W. Chang, A. Ankiewicz, J. M. Soto-Crespo, and N. Akhmediev, "Dissipative soliton resonance as a guideline for high-energy pulse laser oscillators," *J. Opt. Soc. Am. B*, vol. 27, no. 11, Nov. 2010, Art. no. 2336, doi: 10.1364/JOSAB.27.002336.
[16] S.-K. Wang, Q.-Y. Ning, A.-P. Luo, Z.-B. Lin, Z.-C. Luo, and W.-C. Xu, "Dissipative soliton resonance in a passively mode-locked figure-eight fiber laser," *Opt. Express*, vol. 21, no. 2, pp. 2402–2407, Jan. 2013, doi: 10.1364/OE.21.002402.
[17] Y. Wang *et al.*, "Unusual evolutions of dissipative-soliton-resonance pulses in an all-normal dispersion fiber laser," *IEEE Photon. J.*, vol. 11, no. 1, Feb. 2019, doi: 10.1109/JPHOT.2019.2895687.
[18] H. Lin, C. Guo, S. Ruan, and J. Yang, "Dissipative soliton resonance in an all-normal-dispersion Yb-doped figure-eight fibre laser with tunable output," *Laser Phys. Lett.*, vol. 11, no. 8, Jun. 2014, Art. no. 085102, doi: 10.1088/1612-2011/11/8/085102.
[19] H. Xu, S. Chen, and Z. Jiang, "Route to generate high-peak-power dissipative soliton resonance in a nonlinear amplifying loop mirror-based figure-eight laser," *Opt. Eng.*, vol. 58, no. 3, Mar. 2019, Art. no. 036107, doi: 10.1117/1.OE.58.3.036107.
[20] Z.-S. Deng *et al.*, "Switchable generation of rectangular noise-like pulse and dissipative soliton resonance in a fiber laser," *Opt. Lett.*, vol. 42, no. 21, pp. 4517–4520, Nov. 2017, doi: 10.1364/OL.42.004517.
[21] Y. Zhao, P. Guo, X. Li, and Z. Jin, "Ultrafast photonics application of graphdiyne in the optical communication region," *Carbon*, vol. 149, pp. 336–341, Aug. 2019, doi: 10.1016/j.carbon.2019.04.075.
[22] K. Sugioka and Y. Cheng, "Ultrafast lasers—reliable tools for advanced materials processing," *Light Sci. Appl.*, vol. 3, no. 4, pp. e149–e149, Apr. 2014, doi: 10.1038/lsa.2014.30.
[23] J. Liu *et al.*, "Generation and evolution of mode-locked noise-like square-wave pulses in a large-anomalous-dispersion Er-doped ring fiber laser," *Opt. Express*, vol. 23, no. 5, pp. 6418–6427, Mar. 2015, doi: 10.1364/OE.23.006418.
[24] P. Hajireza, W. Shi, K. Bell, R. J. Paproski, and R. J. Zemp, "Non-interferometric photoacoustic remote sensing microscopy," *Light Sci. Appl.*, vol. 6, no. 6, pp. e16278–e16278, Jun. 2017, doi: 10.1038/lsa.2016.278.
[25] D. Li, D. Tang, L. Zhao, and D. Shen, "Mechanism of dissipative-soliton-resonance generation in passively mode-locked all-normal-dispersion fiber lasers," *J. Light. Technol.*, vol. 33, no. 18, pp. 3781–3787, Sep. 2015, doi: 10.1109/JLT.2015.2449874.
[26] Y. Lyu *et al.*, "Multipulse dynamics under dissipative soliton resonance conditions," *Opt. Express*, vol. 25, no. 12, pp. 13286–13295, Jun. 2017, doi: 10.1364/OE.25.013286.
[27] Y. Lyu, H. Shi, C. Wei, H. Li, J. Li, and Y. Liu, "Harmonic dissipative soliton resonance pulses in a fiber ring laser at different values of anomalous dispersion," *Photon. Res.*, vol. 5, no. 6, pp. 612–616, Dec. 2017, doi: 10.1364/PRJ.5.000612.